URSI GASS 2021, Rome, Italy, 28 August - 4 September 2021

Boundary-induced temporal interfaces: analysis of a waveguide-to-waveguide transition

L. Stefanini [(1)], D. Ramaccia, A. Toscano, F. Bilotti
(1) Dept. of Engineering, Roma Tre University, 00146, Rome, Italy
luc.stefanini@stud.uniroma3.it

1 Abstract

Temporal metamaterials are artificial materials whose electromagnetic properties vary over time. An abrupt change of the refractive index over time realizes the so-called *temporal interface*, that induces the generation of a reflected and a refracted wave. In this contribution, we investigate on the possibility to emulate temporal interfaces by acting on the boundary conditions rather than on the material properties. We demonstrate that by suddenly changing the geometrical properties of a waveguide, it is possible to have an equivalent temporal interface, without acting on the material properties. Such an approach opens the door to a simplified exploitation of the properties of temporal interfaces, relaxing the requirements of material modulation.

1 Introduction

In the last years, thanks to the recent possibilities to control the material properties over time, in addition to over space, there was a growing interest on space-time metamaterials [1], [2]. Among them, the class of temporal metamaterials consists of artificial materials whose refractive indices are spatially invariant but vary over time. An abrupt change of the refractive index in the whole space realizes a *temporal interface*, which leads to the generation of a reflected and a refracted wave. This phenomenon was originally investigated by Morgenthaler [3], who considered the scenario of a travelling wave in a medium whose characteristics are abruptly changed over time, realizing simultaneously a frequency shift and the generation of reflected and refracted waves in the new material after the discontinuity. Combining more than one interface opens the door to realizing temporal devices, such as temporal Fabry-Perot cavities and matching slabs [4], antireflection coatings [5], broadband absorbers [6], just to name a few. However, the practical implementation of such a temporal metamaterial is not a straightforward task.
In this contribution, we propose to induce a temporal discontinuity by acting on the boundary conditions of a travelling wave system, rather than on the material properties. The abrupt change of the geometrical properties of the waveguide walls returns a response similar to the one induced by the temporal interfaces, due to the change of the effective refractive index seen by the wave during the propagation. We consider here a conventional parallel-plate waveguide (PPWG), whose metallic plates are at a distance d_1 before the instant of time t_0, and d_2 after it, as illustrated in Fig. 1.

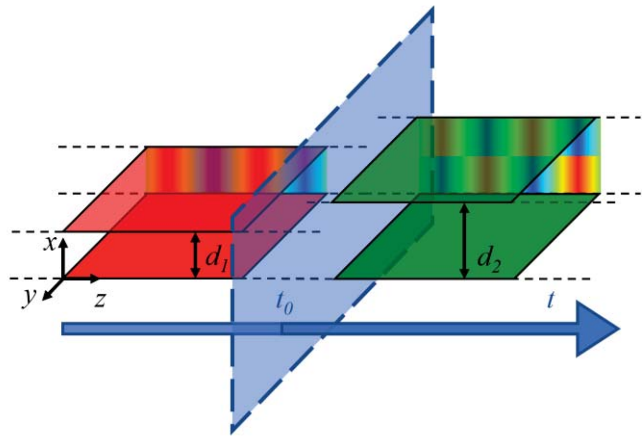

Figure 1. Boundary-induced temporal interface in a parallel plate waveguide. The height of the waveguide is suddenly increased from d_1 to d_2 at the time instant t_0.

In the following sections, we describe in detail the effect induced by the boundary modification in terms of induced frequency shift and coupling with the supported modes of the new waveguide. We report the analytically evaluated transmission and reflection coefficients and compare them with the numerical results.

2 Frequency shift and mode coupling induced by boundaries

Let us consider a PPWG infinitely extended in the *yz*-direction and with height d_1 along the *x*-direction (Fig. 1), operating in a monomodal regime and supporting the propagation of a TM_1 mode. The electromagnetic wave is propagating in the *z*-direction with wavevector k_{z1} at the operative frequency f_0. In Fig. 2a, we report a graphical representation of the dispersion diagram at the frequency f_0 (blue dashed circle) before the temporal boundary discontinuity. For a given height of the waveguide the *x*-component of k_{01}, *i.e.* $\pm k_{x1}$, is set, defining, in turn, the value of k_{z1}. After the temporal discontinuity, the component k_x suddenly changes to k_{x2}, whereas the propagating wavenumber dictated by k_{z1} is maintained. This forces the system to propagate with a different k_0,

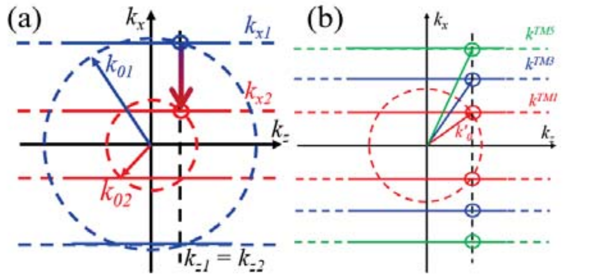

Figure 2. (a) The monomodal and (b) the multimodal case discontinuity induced by the temporal boundary discontinuity at t_0. The presence of a positive and negative k_x is given by the fact that the field distribution can be seen as two propagating waves, having same k_z and opposite k_x, interfering with each other.

i.e., k_{02} (red dashed circle), modifying instantaneously the temporal frequency of the propagating wave.

However, the waveguide after t_0 supports theoretically an infinite number of modes with the same propagation vector $k_z = k_{z1}$, as shown in Fig. 2b. In particular, at the transition, the initial spatial field distribution within the waveguide remains unaltered, but this spatial distribution is no longer an eigen solution for the new structure. Therefore, during the propagation the original mode starts decreasing exponentially and its energy is transferred to the new eigen-modes of the waveguide with the same k_z through a mode coupling mechanism, regardless being forward or backward propagating.

Considering the generic *m*-th circumference in the dispersion diagram in Fig. 2b, the corresponding forward and backward modes propagating in the waveguide exhibit the following temporal frequency:

$$\omega_m = \omega_0 \sqrt{1 - \frac{k_{x1}^2 - k_{xm}^2}{k_{02}^2}} \tag{0.1}$$

The exact amount of energy coupled to each mode from the original one is defined by the phase-matching condition and symmetry-matching between modes. By using coupled mode theory (CMT) together with the time discontinuity boundary conditions, we evaluated in closed form the transmission and reflection coefficients for each mode. The final expressions are reported below:

$$\begin{aligned} T_H &= \frac{k_{xm}}{2k_{x1}} \kappa_{em} \left(1 + \frac{\omega_0}{\omega_m}\right)\left(\frac{\omega_0}{\omega_1}\right) \\ R_H &= \frac{k_{xm}}{2k_{x1}} \kappa_{em} \left(1 - \frac{\omega_0}{\omega_m}\right)\left(\frac{\omega_0}{\omega_1}\right) \end{aligned}, \tag{0.2}$$

where ω_1 is the frequency of the first mode in the new structure and κ_{em} is the coupling coefficient given by the overlap integral across the PPWG cross section.

3 Numerical verification

In this section, we verify the temporal interface induced by the boundary change over time, evaluating numerically the

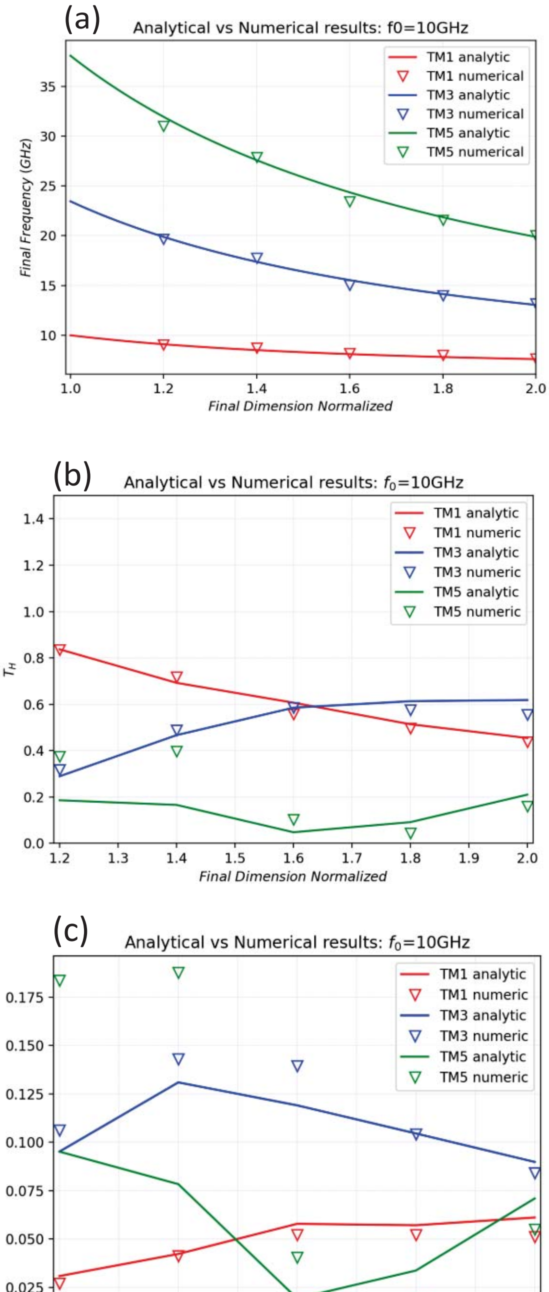

Figure 3. The source central frequency is set at 10 GHz and the frequency content spans 2 GHz in both directions; the initial height was 2 cm and the final height after the abrupt temporal change is sampled every 0.4 cm. On the horizontal axis we report the height normalized to the initial one. From top to bottom we plot the expected frequency shifts (a), the transmission coefficients (b), and the reflection coefficients (c). Solid lines refer to the analytical results, while the triangles to the numerical ones.

frequency shift and the corresponding reflection and transmission coefficients for the induced modes after the temporal discontinuity. We developed a finite difference time domain (FDTD) numerical code [7]-[8] to simulate over time the propagation and transformation of the original mode into the final set of forward and backward propagating modes in the PPWG.

In the simulation, we consider a PPWG height of 2 cm, supporting the propagation of the lowest order TM mode at 10 GHz. Five different simulations have been performed, where the temporal interface is induced by the boundary modification from 2 cm to 2.4, 2.8, 3.2, 3.6, 4.0 cm, respectively.

In Fig 3a, we report the comparison between the analytical (solid line) and numerical (symbols) results in terms of the frequency shifts for the first three odd modes, *i.e.,* TM_1, TM_3, TM_5, showing that even for the lowest order mode the boundary-induced temporal transition changes its frequency, slightly reducing it from the original one $f_0=10$ *GHz.*

In Figs. 3b-c, we report the amplitude of the reflection and transmission coefficients at the boundary-induced temporal interface for the modes after the waveguide discontinuity. The results present very good agreement except for the TM_5 mode when small jumps in the waveguide height are considered. This is just due to the finite resolution of our simulation that hardly catches the high frequency responses of the TM_5 mode for such a boundary jump. However, for wider jumps, which corresponds to lower frequency shifts, the results are in line again with what we expected form the theoretical analysis.

4 Conclusions

To conclude, we demonstrated that it is possible to achieve a temporal interface by acting on the boundaries of a guiding structure. We presented a brief theoretical explanation of the phenomenon followed by the closed form solution for the frequency shifts and the energy distribution for each forward and backward mode. Those preliminary results can clear the path for the implementation of a device based on a time interface, relaxing the need of directly modulating the material properties.

4 References

[1] C. Caloz and Z.-L. Deck-Léger, “Spacetime Metamaterials — Part I : General Concepts,” *IEEE Trans. Antennas Propag.*, vol. 68, no. 3, pp. 1569–1582, 2020.

[2] C. Caloz and Z.-L. Deck-Léger, “Spacetime Metamaterials—Part II: Theory and Applications,” *IEEE Trans. Antennas Propag.*, vol. 68, no. 3, pp. 379–381, 2020, doi: 10.1109/metamaterials49557.2020.9285025.

[3] R. Morgenthaler, “Velocity Modulation of Electromagnetic Waves,” *IRE Trans. Microw. Theory Tecnhiques*, 1958.

[4] D. Ramaccia, A. Toscano, and F. Bilotti, “Light propagation through metamaterial temporal slabs: Reflection, refraction, and special cases,” *Opt. Lett.*, vol. 45, no. 20, 2020, doi: 10.1364/OL.402856.

[5] V. Pacheco-Peña and N. Engheta, “Anti-reflection temporal coatings,” *Optica*, vol. 7, no. 4, pp. 323–331, Mar. 2020, doi: 10.1364/optica.381175.

[6] H. Li and A. Alù, “Temporal switching to extend the bandwidth of thin absorbers,” *Optica*, vol. 8, no. 1, p. 24, Jan. 2021, doi: 10.1364/optica.408399.

[7] H. P. Langtangen, “Finite difference methods for wave motion,” pp. 1–108, 2013.

[8] J. C. Strikwerda, *Finite Difference Schemes and Partial Differential Equations, Second Edition*. Society for Industrial and Applied Mathematics, 2004.